Space-time Fourier Ptychography for *in vivo* Quantitative Phase Imaging

جامعة الملك عبدالله للعلوم والتقنية
King Abdullah University of Science and Technology

Ming Sun, Kunyi Wang, Yogeshwar Nath Mishra, Simeng Qiu, and Wolfgang Heidrich*

Visual Computing Center, King Abdullah University of Science and Technology (KAUST), Thuwal 23955-6900, Saudi Arabia

جامعة الملك عبدالله للعلوم والتقنية
King Abdullah University of Science and Technology

INTRODUCTION

Space-Time Fourier Ptychography (ST-FP)

Challenge: Imaging dynamic, constantly moving biological specimens.

Solution: Combines rapid Fourier Ptychography with space-time motion priors.

Key Features:

- **Increased SBP-T:** Increases the space-time bandwidth product of the reconstructed complex image sequence while leveraging redundant temporal information to achieve robust reconstruction.
- **Applications:** Ideal for observing rapid morphological changes in living organisms and reconstructing moving amplitude and phase targets.

METHODS

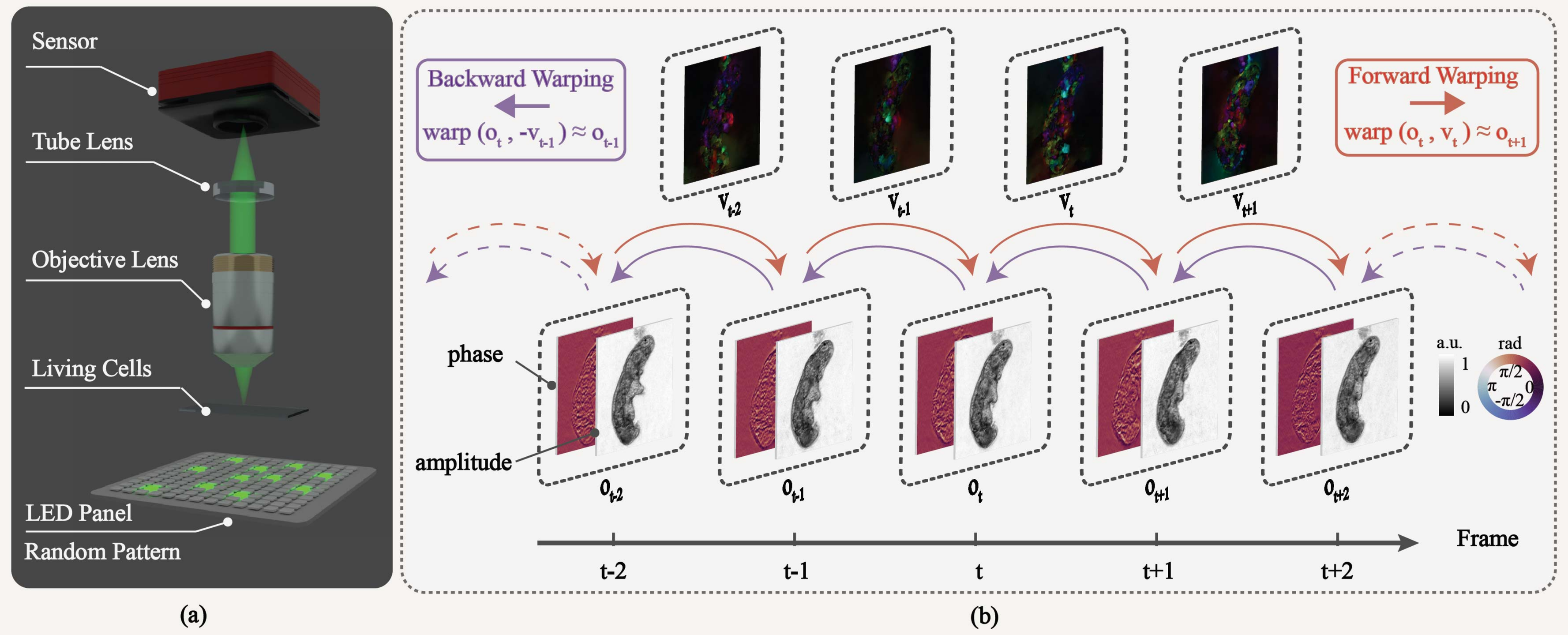

Principle of Space-time Fourier Ptychography (ST-FP). (a)Schematic of ST-FP setup, including multiplexed LED illumination and the pathway through lenses to the sensor, captures the dynamics of living organisms. (b) To address rapid deformations between successive frames, a novel reconstruction approach utilizes warping to approximate intermediate frame states. For each time stamp, raw data $\mathbf{b}_t$ is captured under multiplexed illumination. Utilizing motion fields $-\mathbf{v}_{t-1}$ and $-\mathbf{v}_t$, backward and forward warping are applied to estimate $\mathbf{b}_{t-1}$ and $\mathbf{b}_{t+1}$, respectively. This approach effectively aggregates phase and amplitude information across time, resulting in increased reconstruction accuracy and resolution. This method aligns each captured raw frame with its temporal stamp, allowing for the reconstruction of objects even with significant motion, as opposed to the traditional scheme that requires negligible object movement.

Forward Model

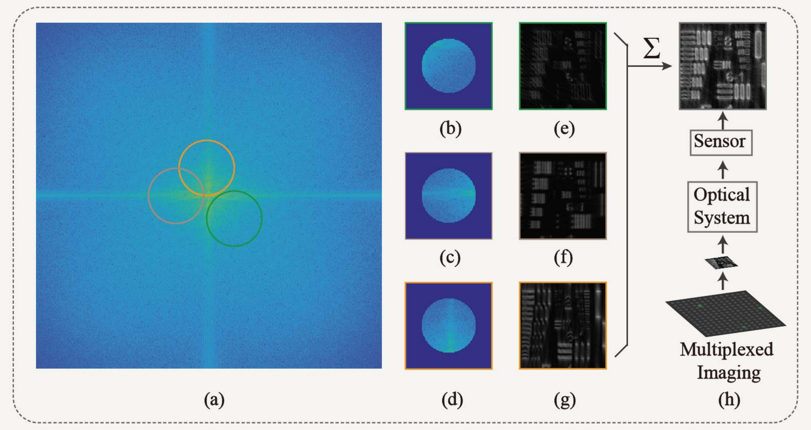

Schematic of Fourier Ptychography (FP) with multiplexed illumination.
(a) A single low-resolution (LR) image captured under a specific LED pattern, is indicative of the spatial frequency information of the object. (b)-(d) Resultant frequency domain representations, showing the spatial frequency shifts induced by different illumination angles. (e)-(g) Sub-images corresponding to different spatial frequency regions obtained under varied LED illuminations. (h) The imaging system schematic illustrates the pathway from multiplexed illumination to the sensor.

ST-FP Framework

$$
\begin{aligned}
\min_{\{\mathbf{o}_t,\mathbf{v}_t\}_t} & \sum_{t=1}^{T}\left\|\mathscr{A}_t(\mathbf{o}_t)-\mathbf{b}_t\right\|_2^2+\alpha\sum_{t=1}^{T-1}\left\|\mathbf{D}_t|\mathbf{o}_t|+\mathbf{D}_s|\mathbf{o}_t|\cdot\mathbf{v}_t\right\|_2^2 \\
& +\gamma\left(\sum_{t=1}^{T-1}\left\|\mathscr{A}_{t+1}(\mathrm{warp}(\mathbf{o}_t,\mathbf{v}_t))-\mathbf{b}_{t+1}\right\|_2^2+\sum_{t=2}^{T}\left\|\mathscr{A}_{t-1}(\mathrm{warp}(\mathbf{o}_t,-\mathbf{v}_{t-1}))-\mathbf{b}_{t-1}\right\|_2^2\right) \\
& +\beta\sum_{t=1}^{T-1}\left(\left\|\mathbf{D}_s\mathbf{v}_{t,x}\right\|_{H_{\mu 1}}+\left\|\mathbf{D}_s\mathbf{v}_{t,y}\right\|_{H_{\mu 1}}\right)+\delta_1\sum_{t=1}^{T}\left\|\mathbf{D}_s\mathbf{o}_t\right\|_{H_{\mu 2}}+\delta_2\sum_{t=1}^{T-1}\left\|\mathbf{D}_t\mathbf{o}_t\right\|_{H_{\mu 3}}
\end{aligned}
$$

The first term is the data fidelity term for the individual measurements. $\mathscr{A}_t(\cdot)$ is the forward multiplexing function for frame t, $\mathbf{o}_t$ is the (complex-valued and \emph{moving}) object at time t, and $\mathbf{b}_t$ represents the observed measurement.
The second term is the optical flow term that jointly estimates the velocity / motion of the object. $\mathbf{D}_t$ and $\mathbf{D}_s$ are the temporal and spatial discrete gradient operators, implemented as one-sided divided differences. $\mathbf{v}_t$ is the velocity field estimated for the motion from the amplitude image $|\mathbf{o}_t|$ to amplitude image $|\mathbf{o}_{t+1}|$.
The next line incorporates the warp-and-project method, in which the partial reconstruction of the object at time t is warped forward (and backward) in time, undergoes the image formation model $\mathscr{A}_{t+1}$ at that time (project), the result of which is compared to the measurement $\mathbf{b}_{t+1}$ obtained for that time.
The final line has several smoothness regularizers for both the motion field (in space) and the object (in space and time). For these smoothness terms we utilize the Huber penalty function $\|\cdot\|_H$, which provides a tradeoff between the l1 and l2 norms. $\gamma,\alpha,\beta,\delta_1$ and δ_2 are weights of the different terms.

RESULTS

Simulation Results

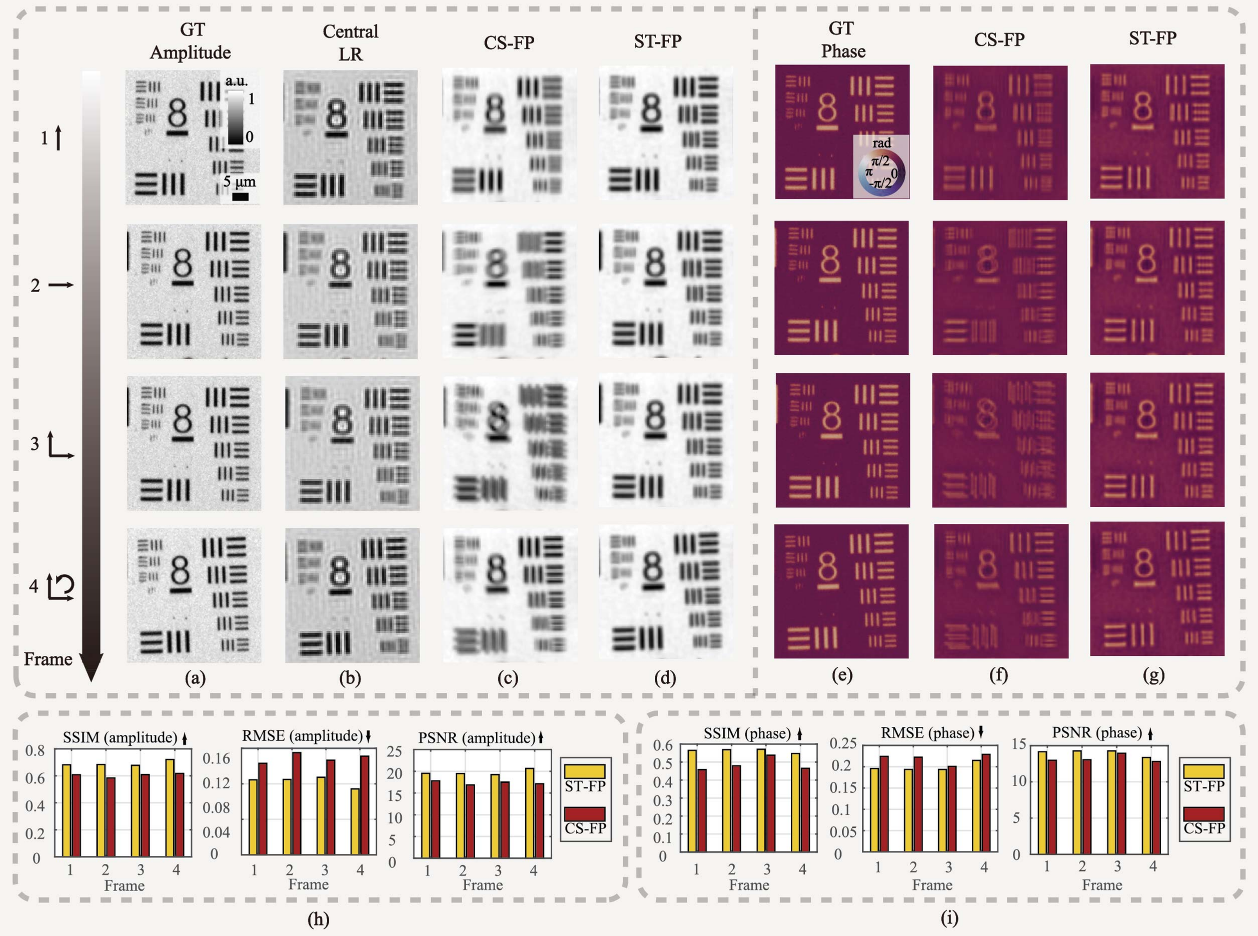

Comparative analysis of dynamic simulation across four frames using for a complex-valued USAF target. Frames simulate distinct motion types: translations along the y-axis, x-axis, combined x-y axes, and a composite translation-rotation motion. (a) Ground truth (GT) for amplitude. (b) LR sub-image under central FP system illumination. (c-d) Amplitude reconstruction for CS-FP and proposed ST-FP. (e) GT for phase. (f) and (g) are phase results of CS-FP and ours. (h) and (i) Comparison of amplitude and phase reconstruction quality against the GT, using SSIM, RMSE, and PSNR metrics for both CS-FP and ST-FP.

Amplitude simulation results (USAF target)

	SSIM ↑		RMSE ↓		PSNR ↑	
Frame	ST-FP	CS-FP	ST-FP	CS-FP	ST-FP	CS-FP
1	**0.6822**	0.6087	**0.1056**	0.1288	**19.5294**	17.8000
2	**0.6838**	0.5837	**0.1061**	0.1439	**19.4861**	16.8406
3	**0.6778**	0.6090	**0.1092**	0.1333	**19.2349**	17.5047
4	**0.7211**	0.6172	**0.0928**	0.1390	**20.6487**	17.1415

Phase simulation results (USAF target)

	SSIM ↑		RMSE ↓		PSNR ↑	
Frame	ST-FP	CS-FP	ST-FP	CS-FP	ST-FP	CS-FP
1	**0.5651**	0.4581	**0.1957**	0.2242	**14.1667**	12.9873
2	**0.5690**	0.4792	**0.1936**	0.2225	**14.2625**	13.0537
3	**0.5710**	0.5385	**0.1935**	0.2007	**14.2679**	13.9490
4	**0.5476**	0.4652	**0.2147**	0.2288	**13.3631**	12.8106

Experiments with Controlled Motion

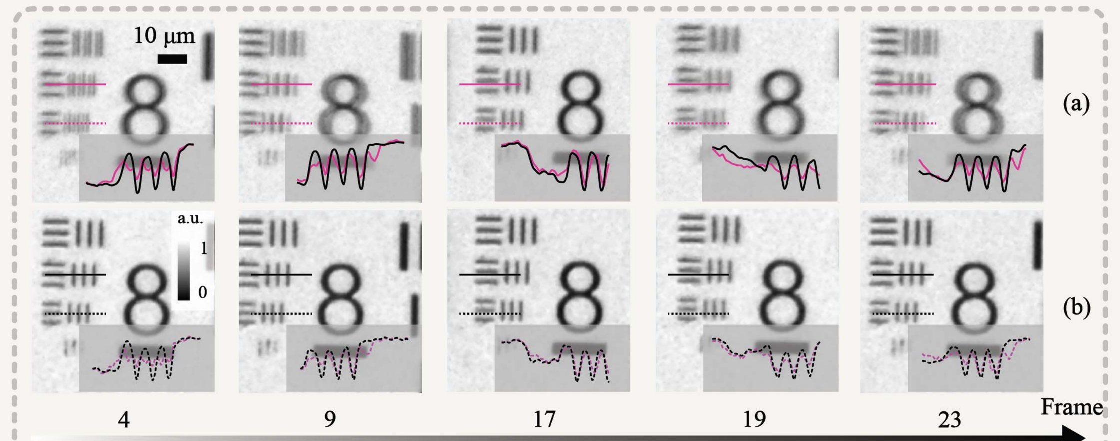

Comparative analysis using moved pure amplitude USAF target.
(a) The sequence of results under dynamic conditions by CS-FP. (b) The sequence of images by ST-FP

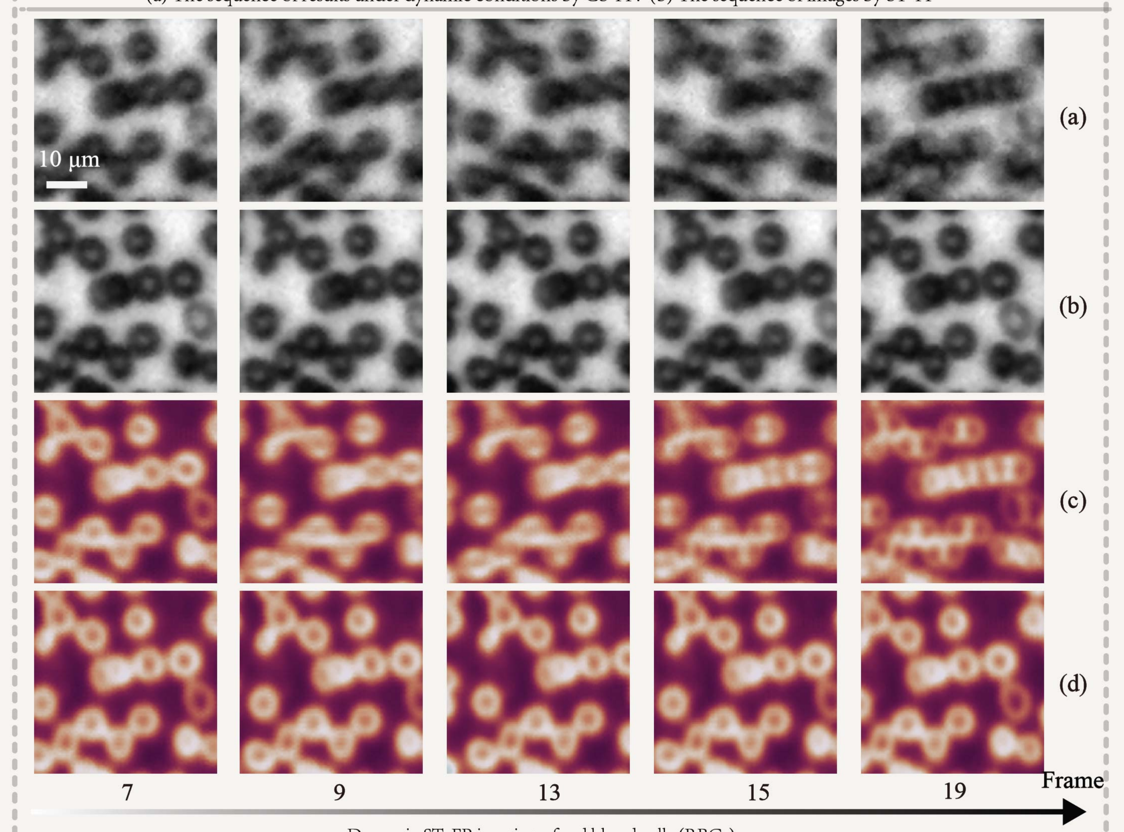

Dynamic ST-FP imaging of red blood cells (RBCs).
(a) and (c) Temporal amplitude and phase results by CS-FP method. (b) and (d) Corresponding results by ST-FP.

Experiments with Uncontrolled Motion (Live Microorganisms)

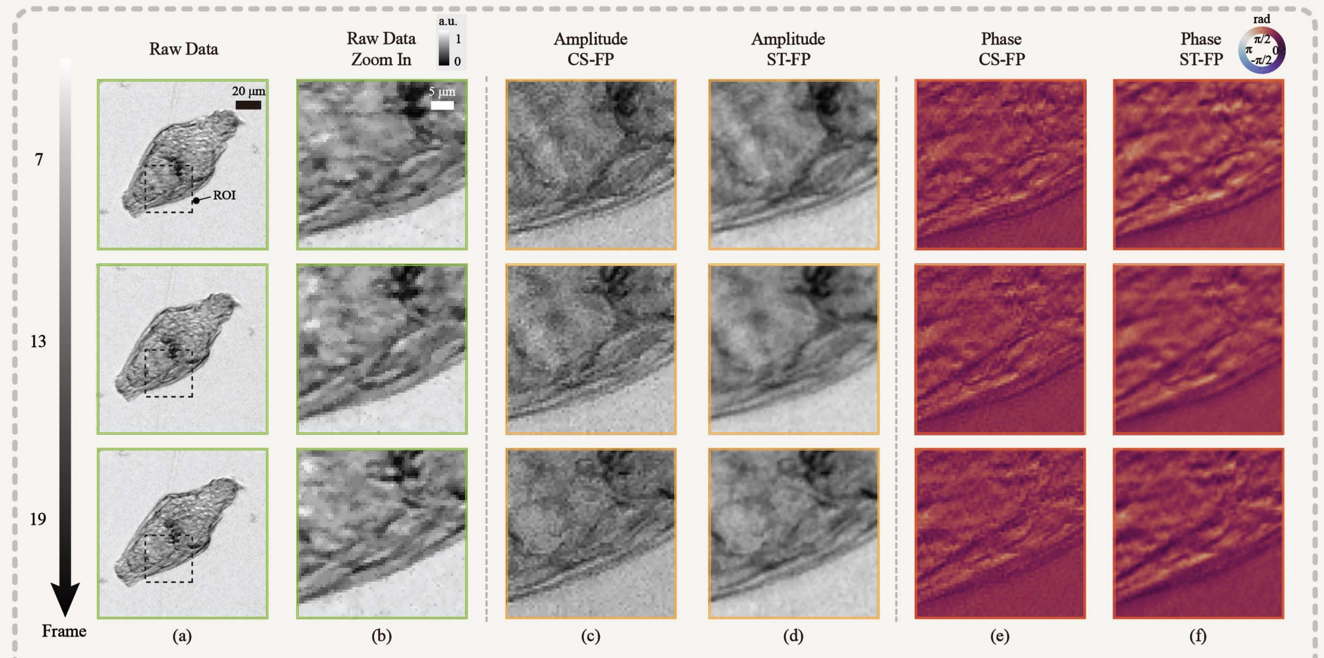

Results comparison of a live rotifer at different times.
(a) LR raw data. (b) ROI from (a). (c) and (d) are amplitude results of CS-FP and our method. (e) and (f) are phase results of CS-FP and our method.

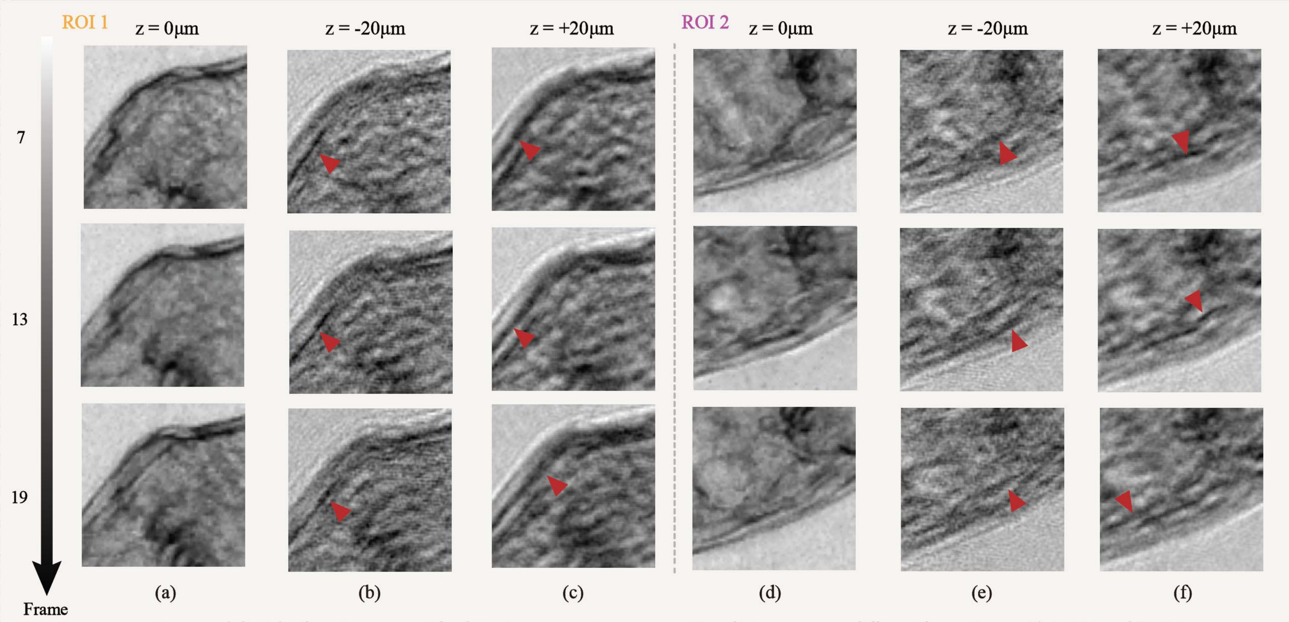

Temporal digital refocusing on a rotifer dataset across various propagation distances across different frame times with ROI 1 and ROI 2.

ABLATION STUDY (CS-FP)

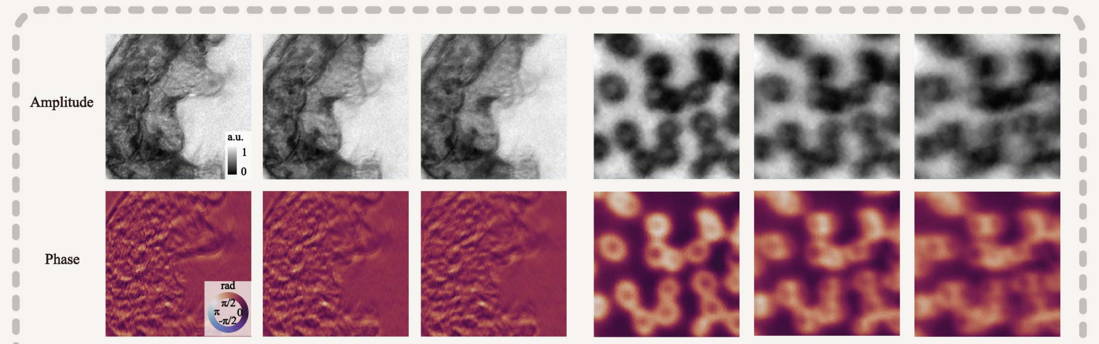

Comparative Analysis of CS-FP by different image quantities for object reconstruction.
(a)-(c) Results of a tardigrade reconstructed using 2, 3, and 4 of CS-FP respectively. (d)-(f) Results of moving RBCs reconstructed with different numbers of images.
The two-image approach is shown to significantly reduce the blurring effect, yielding the clearest results.

REFERENCES

[1] G. Zheng, R. Horstmeyer, and C. Yang, “Wide-field, high-resolution Fourier ptychographic microscopy,” Nat. Photonics 7, 739–745 (2013).
[2] G. Zang, R. Idoughi, R. Tao, et al., “Warp-and-project tomography for rapidly deforming objects,” ACM Trans. Graph. 38 (2019).
[3] G. Zang, R. Idoughi, R. Tao, et al., “Space-time tomography for continuously deforming objects,” ACM Trans. Graph. 37 (2018).
[4] X. Li, L. Li, X. Liu, et al., “Dictionary-based compressive Fourier ptychography,” Opt. Lett. 47, 2314–2317 (2022).

ACKNOWLEDGMENTS

The authors thank Dr. Qiang Fu and Dr. Hadi Amata from Visual Computing Center at King Abdullah University of Science and Technology for constructive discussions and sample fabrication support.